Advanced Powder Technology 30 (2019) 2541–2547

Contents lists available at ScienceDirect

Advanced Powder Technology

journal homepage: www.elsevier.com/locate/apt

Original Research Paper

Experimental investigation on the packed bed of rodlike particles

Wenguang Nan [a,*], Yueshe Wang [b], Houhuan Sun [a]

[a] School of Mechanical and Power Engineering, Nanjing Tech University, Nanjing 211816, China
[b] State Key Laboratory of Multiphase Flow in Power Engineering, Xi'an Jiaotong University, Xi'an 710049, China

ARTICLE INFO

Article history:
Received 24 May 2019
Received in revised form 20 July 2019
Accepted 31 July 2019
Available online 12 August 2019

Keywords:
Rodlike particle
Non-spherical particle
Packing
Friction factor
Fluidisation

ABSTRACT

Rodlike particles have been usually found in industrial applications, such as the straw and needle catalyst in energy and chemical engineering. Compared to spherical particles, rodlike particles exhibit different behaviour in the packing structure due to their rotational movement. In this work, we have experimentally explored the packing structure and its friction factor for fluid flow. The porosity of packing structure generated by two packing methods is measured for four kinds of rodlike particles. The experimental results show that the porosity of bed of rodlike particles in the poured packing is not a monotonic function of the aspect ratio of particles. This is due to the competition between the "self-fitting" effect and excluded effect. The porosity of bed of rodlike particles is more sensitive to the packing method than that of spherical particles. To describe the pressure drop of fluid flow through the packing structure, the Ergun equation is further modified by introducing the modified Reynolds number and Galileo number. By combing the experimental data for packed bed generated by the fluidised packing method, and other experimental work in current literature, a new empirical equation is proposed to predict the friction factor of the packing structure of rodlike particles, in which the effects of the particle orientation and particle shape are both considered by the equivalent sphericity. These experimental results would be of interest from applied standpoints as well as revealing fundamental effects of the aspect ratio of rodlike particles on the packing structure.

1. Introduction

Rodlike particles have been widely used in many industrial applications, such as the straw in biomass utilization and the needle catalyst in chemical and pharmic engineering. During the processes such as fluidisation and catalytic reaction, the pressure drop and heat transfer of fluid flow as well as catalytic efficiency are strongly affected by the porosity and the friction behaviour of the packed bed. Compared to spherical particles, rodlike particles exhibit unique behaviours, such as the rotational movement and anisotropic distribution of particle orientation. However, the structure of the packed bed of rodlike particles up till now is still lacking for rigorous elucidation. In order to generate sufficient information for general applications, it is essential and practical to illustrate the packing structure of rodlike particles and the friction behaviour of fluid flow.

For the packed bed of rodlike particles, several researchers [1–8] had experimentally measured the porosity, and showed that the porosity strongly depended on the aspect ratio. For example, Novellani et al. [7] found that the porosity of bed could increase from 0.42 to 0.90 when the aspect ratio changed from 5 to 50. Based on these experimental results, Parkhouse & Kelly [4], Zou & Yu [5] and Rahli et al. [6] also proposed several empirical correlations to predict the porosity of bed of rodlike particles. Besides the porosity of bed in the experiments, the microscopic structural information could be further extracted by numerical simulation [9–17], such as the coordination number and particle orientation. Williams and Philipse [9] found that the spatial correlations gradually vanished with increasing the aspect ratio. Zhao et al. [12] simulated the densely random packing of spherocylinders by using an improved geometric-based relaxation algorithm, and showed that the coordination number was not a monotonic function of the aspect ratio. Meng et al. [13] simulated the packed bed of the mixtures of rodlike particles with different aspect ratios, and proposed an empirical correlation to predict the porosity of bed of mixtures. Nan et al. [16] confirmed the strong tendency of horizontal alignment of rodlike particles in the packed bed. However, as different packing methods are used in these work, the underlying mechanism of the effect of aspect ratio on the packing structure is still needed to be further explored.

* Corresponding author.
E-mail address: nanwg@njtech.edu.cn (W. Nan).

https://doi.org/10.1016/j.apt.2019.07.034

The fluid flow through the packed bed of non-spherical particles had been explored by several researchers through experiments [18–26] and numerical simulations [27–37]. Among these work, only limited information was related to rodlike particles. Nemec & Levec [20] experimentally measured the pressure drop of fluid flow through the packed bed of spherical particles as well as rodlike particles (l/d = 1.31, 2.94, 5.77), and proposed an empirical correlation to predict the pressure drop. Liu [23] measured the minimum fluidisation velocity of cylinders, and showed that the minimum fluidisation velocity was smaller than that of spherical particles. Allen et al. [25] showed that the pressure drop of fluid flow through the packed bed of rodlike particles was much different to that of spherical particles, and also developed another empirical equation to predict the pressure drop, which was based on the experiment result of only one kind of rodlike particles (l/d = 1.2). By using DEM-CFD simulation, Zhong et al. [27] simulated the fluidised behaviour of rodlike particles (l/d = 2.3), including the bed expansion ratio and particle volume fraction. Oschmann et al. [32] claimed that rodlike particles tended to mix slower with increasing elongation if the same gas velocity was applied. Vollmari et al. [33,34] compared the simulation results with their experimental work, and showed that the particle orientation had a great influence on the pressure drop. Nan et al. [35] also simulated the minimum fluidisation velocity and the fluidised behaviour of spherical particles as well as two kinds of rodlike particles (l/d-1 = 5.0 and 8.0), and showed that there should be a minimum U_{mf} for rodlike particles as the particle sphericity decreases. Due to the limit of the experiment work on the fluid flow through the packed bed, the empirical correlations of the friction factor are defective.

In this work, the porosity and the friction factor of the packed bed of rodlike particles are investigated by experiments. The packed bed is generated by two methods, and the variation of the porosity with aspect ratio is illustrated with the underlay mechanisms. The pressure drop of fluid flow through the packed bed is then explored, and a new empirical equation of the friction factor is developed for the packed bed of rodlike particles.

2. Particle characterisation

In this work, to investigate the effect of aspect ratio of particles on the structure of the particle bed, four kinds of rodlike particles with different aspect ratios are used. Two kinds of rodlike particles are made from ceramic with white colour, which are designated as WS and WL, respectively; and another two are accurately cut from long carbon fibres with black colour, which are designated as BS and BL, respectively. Besides rodlike particles, the spherical glass beads are also used for comparison and designated as GB.

The particle density is measured by the liquid pycnometre method [38,39], where an electric balance with precision of 0.01 g, a 250 mL pycnometre and deionized water are used. The glass beads (GB) have uniform size distribution with diameter of 2 mm. The physical size of rodlike particles is measured by the image analysis method: (1) the particle sample is randomly dispersed on a plate (i.e. black plate for WS and WL particles, white plate for BS and BL particles), and a ruler is fixed onto the plate; (2) the image of the dispersed particles is taken by the camera with high resolution; (3) the physical size per unit pixel of the image is measured based on the scale on the ruler; (4) the background colour is subtracted from the image and the region of ruler in the image is also cut off; (5) the image is binarised, as shown in Fig. 1, and then the size of all particles could be auto-calculated and averaged. By repeating the processes (1)-(5), totally 3–5 samples with around 1000 particles are measured for each kind of rodlike particles.

The particle density and size are shown in Table 1, where the aspect ratio is defined as:

$$AR = l/d - 1 \tag{1}$$

where l and d are the length and diameter of the circular cross-section of particles, respectively. For spherical particles, l is the same as d, and the aspect ratio is zero. For rodlike particles, BS and BL particles have larger aspect ratios than that of WS and WL particles, and the largest aspect ratio is 6.34. Table 1 also shows that the standard deviation of the aspect ratio of particles increases with AR. The probability distribution of the aspect ratio of rodlike particles is close to Gaussian distribution, as shown in Fig. 2.

3. Porosity of the packed bed

The structure of the particle bed is firstly characterised by the porosity, which is defined as:

$$\varepsilon = 1 - \frac{\sum V_p}{V_c} \tag{2}$$

where $\sum V_p$ is the total particle volume, calculated from the particle density and particle mass; V_c is the total volume of the packed bed. To investigate the variation of porosity in different packing conditions, two methods are used to generate the packed bed:

(1) Poured packing. The packed bed is formed by dropping the particles from a specified height and the following sedimentation of particles under gravity. To make the measurement have good repeatability, two plexiglass cylinders with the same diameter of 100 mm are used. They are firstly put together in the vertical direction, and the top one (i.e. hollow cylinder vessel) is then slowly removed along horizontal direction when the packed bed is generated, resulting in the final bed with a flat surface. The porosity of bed could be calculated from the weighted mass of the final packed bed and the volume of the bottom cylinder vessel.
(2) Fluidised packing. The particles are poured into a rectangular vessel and then the particle bed is fully fluidised. By slowly decreasing the superficial gas velocity, the fluidised bed could pack again under gravity and air drag, resulting in a new particle bed with a smooth free surface. The porosity of bed is calculated based on the height of the new particle bed, which could be obtained from the image analysis method.

The variation of the porosity with the aspect ratio of particles is shown in Fig. 3. It shows that the porosity of bed strongly depends on the aspect ratio of particles, and the packed bed formed by particles with larger aspect ratio is usually looser than that with smaller aspect ratio. Comparing two methods, a denser packed bed could be obtained in the poured method. For the spherical glass beads, the difference of porosity of bed between these two methods is much smaller than that of rodlike particles. It indicates that the porosity of bed of rodlike particles is more sensitive to the packing method than that of spherical particles.

Fig. 3 also shows that in the poured packing method, the minimum porosity of bed does not occur at AR = 0.0 (i.e. spherical particles). With the increase of aspect ratio, the porosity of bed decreases first and then increases. This trend is caused by the competition between two effects:

(1) Rodlike particles could rotate with freedom of 2, and the physical sizes in the axial and radial directions are different. Thus, they could rotate and fit themselves into the surrounding pores in one specified orientation, resulting in

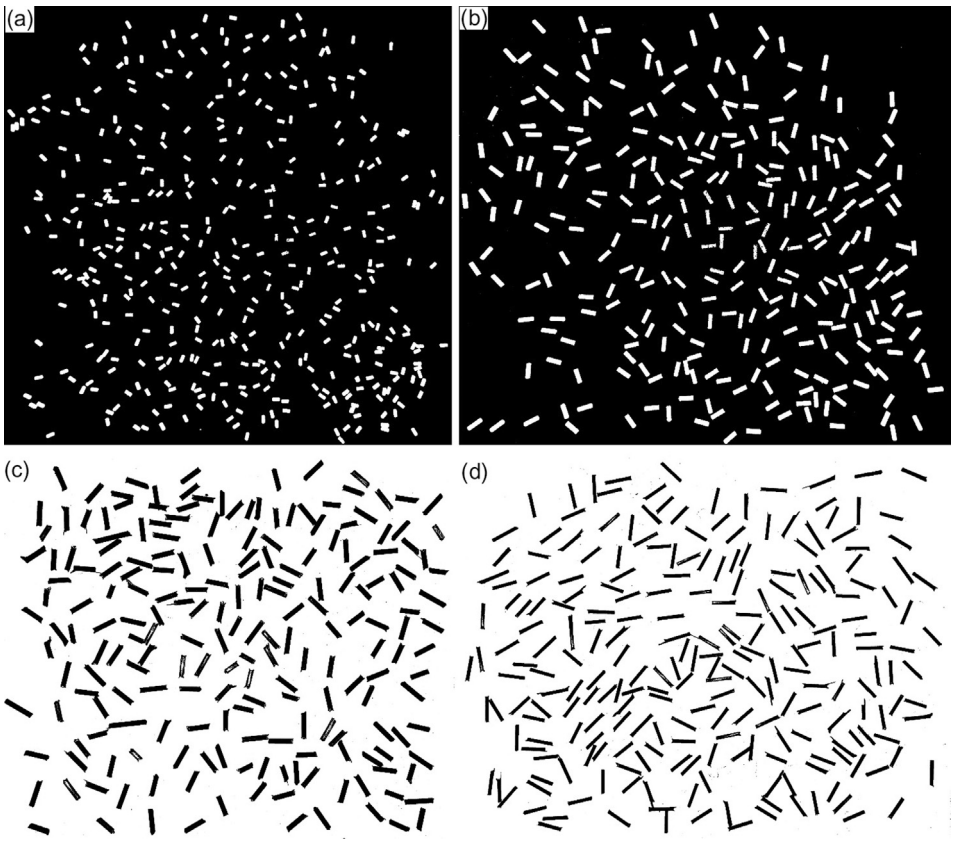

Fig. 1. The snapshots after the binarization of the images of dispersed rodlike particles (a) WS particles; (b) WL particles; (c) BS particles; (d) BL particles.

Table 1
Physical properties of the particles in the experiment.

Label	Material	Density ρ_p/kg·m^{-3}	Length l/mm	Diameter d/mm	Aspect ratio l/d-1
GB	glass	2505	2	2	0
WS	ceramic	3365	3.06 ± 0.14	1.46 ± 0.11	1.11 ± 0.14
WL	ceramic	3230	5.92 ± 0.22	1.84 ± 0.16	2.23 ± 0.24
BS	carbon fibre	1467	11.28 ± 1.54	2.51 ± 0.33	3.53 ± 0.68
BL	carbon fibre	1525	10.92 ± 1.00	1.52 ± 0.33	6.34 ± 0.95

*± is standard deviation.

more efficient packing. This effect is designated as self-fitting effect. It is also similar to the packing of spherical particles with a wide size distribution, where a denser packing structure could be obtained than that of mono-sized spheres. Thus, compared to spherical particles, denser packing of rodlike particles are formed, resulting in more contacts per particle to eliminate the additionally rotational freedom [40].

(2) 2) When the aspect ratio is large enough, the particles which would like to insert into surrounding pores are easily excluded by the surrounding particles, and the free space of motion is also much limited, leading to looser packing structure. This effect is designated as the excluded effect and becomes more pronounced for particles with larger aspect ratio. It could also be quantified by excluded volume of particles [41].

However, in the fluidised packing method, the particle motion is strongly affected by the drag force, and the additional kinetic energy needed for particle rotation and insertion is minimised by slowly decreasing the superficial gas velocity. Thus, the self-fitting effect is limited, and the porosity of bed does not change much when the aspect ratio is small. This trend also agrees well with the DEM simulation results [42], where the AR-ε curve becomes more and more flat with the decrease of the settling velocity when the aspect ratio is small. It also suggests that in different packing methods, the porosity of bed could have different trends with the increase of aspect ratio of particles.

4. Friction factor of the packed bed

According to the pore conduct model [43], the geometry of the packed bed could be simplified as a series of connected conduits with different diameters and lengths, and the pressure drop of fluid flow through the packed bed could be related to the frictional (laminar or turbulent) energy losses along the straight sections of each conduit and the local losses due to the expansions and contractions between each two connected conduits. Based on this hypothesis, the pressure drop of fluid flow through the packed bed could be given as:

$$\frac{\Delta P}{L} = A\frac{\mu(1-\varepsilon)^2}{d_{SV}^2\varepsilon^3}U + B\frac{\rho_f(1-\varepsilon)}{d_{SV}\varepsilon^3}U^2 \tag{3}$$

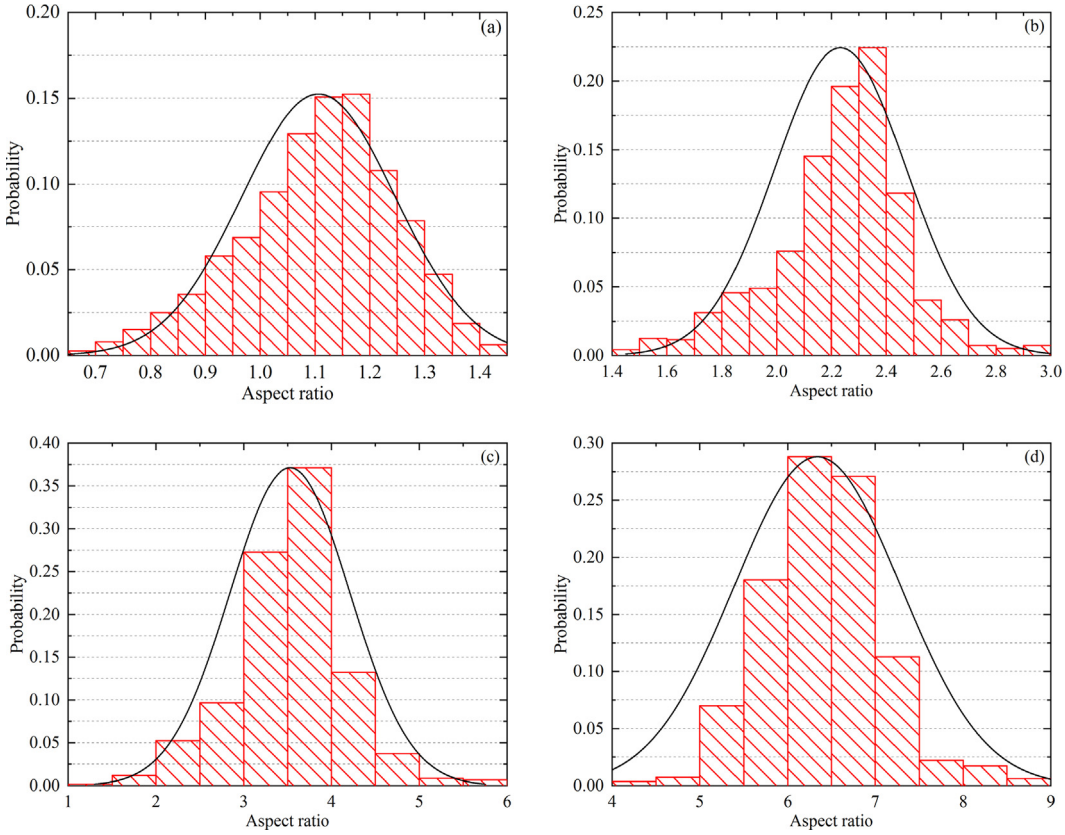

Fig. 2. The probability distribution of the aspect ratio (l/d-1) of rodlike particles (a) WS particles; (b) WL particles; (c) BS particles; (d) BL particles.

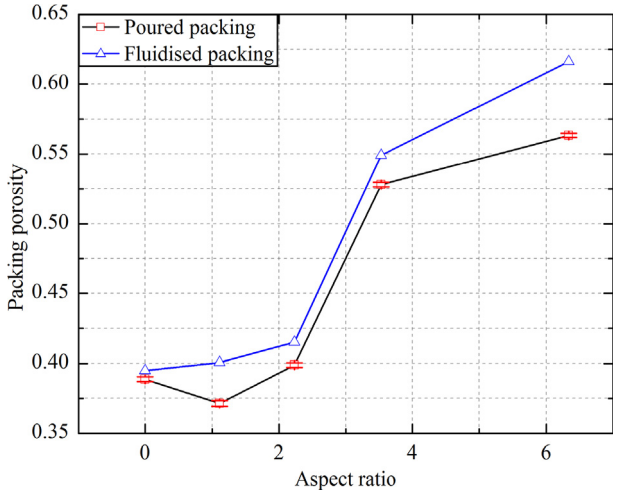

Fig. 3. Variation of the porosity of bed with the aspect ratio (l/d-1) of particles.

where μ is the fluid viscosity; ρ_f is the fluid density; d_{SV} is the Sauter diameter of particles; A and B are constants, depending on the tortuosity of the packed bed, which is the ratio of the length of actual fluid path to that of the packed bed. The first item of the right part arises from the losses of viscous energy, proportional to fluid velocity, and the second item of the right part arises from the local and inertial losses of energy, proportional to the square of fluid velocity.

To apply this equation to the packed bed of rodlike particles, the modified Reynolds number Re^* and Galileo number Ga^* are introduced in this work:

$$Re* = \frac{\rho_f D_e U_e}{\mu} = \frac{\rho_f d_{SV} U}{\mu(1-\varepsilon)} \tag{4}$$

$$Ga* = \frac{\rho_f^2 g D_e^3}{\mu^2} = \frac{\rho_f^2 g d_{SV}^3 \varepsilon^3}{\mu^2 (1-\varepsilon)^3} \tag{5}$$

where D_e and U_e are the characteristic diameter and velocity, respectively:

$$D_e = \frac{6V_{void}}{A_{void}} = \frac{\varepsilon d_{SV}}{(1-\varepsilon)} \tag{6}$$

$$U_e = \frac{U}{\varepsilon} \tag{7}$$

where V_{void} and A_{void} are the volume and surface area of the voids of packed bed, respectively. Thus, Eq. (3) could be written as:

$$\frac{\Delta P/L}{\rho_f g} = \frac{1}{Ga*}(ARe* + BRe*^2) \tag{8}$$

It could be further simplified as:

$$f* = \frac{\Delta P}{L}\frac{d_{SV}}{\rho_f U^2}\frac{\varepsilon^3}{(1-\varepsilon)} = \frac{\Delta P/L}{\rho_f g}\frac{Ga*}{Re*^2} = \frac{A}{Re*} + B \tag{9}$$

where the left part f^* is designated as the friction factor of the packed bed. Although the porosity of bed does not solely appear in Eq. (9), its effect on the pressure drop could be considered by Re^* and Ga^*. Further physical meaning of the derivation of Eqs. (3) and (9) could be found in Niven [43]. The current empirical models of pressure drop of fluid flow through the packed bed in the articles are all converted into the form of Eq. (9) in this work, which are not the original form if not specified.

For spherical particles, the pressure drop could be predicted by Ergun Equation [44]:

$$\Delta P = 150\frac{\mu L}{\phi^2 d_V^2}\frac{(1-\varepsilon)^2}{\varepsilon^3}U + 1.75\frac{\rho_f L}{\phi d_V}\frac{(1-\varepsilon)}{\varepsilon^3}U^2 \tag{10}$$

where the regular sphericity Φ is the ratio between the surface area of the volume equivalent sphere and the considered rod; d_V is the volume-equivalent diameter of particles, which is also equal to d_{SV}/Φ. By converting Ergun equation into Eq. (9), the friction factor could be given as:

$$f* = \frac{150}{Re*} + 1.75 \tag{11}$$

For rodlike particles, Nemc & Levec [20] measured 3 kinds of particles with different aspect ratios (l/d = 1.91, 2.94, 5.77). By combing their own experiment work and the experiment data of Pahl [18] for another two kinds of rodlike particles (l/d = 1.31, 3.81), the dependence of A and B on the particle sphericity could be described by Eqs. (12) and (13) based on data fitting method, which is designated as "N-I" model.

$$A = \frac{150}{\phi^{3/2}} \tag{12}$$

$$B = \frac{1.75}{\phi^{4/3}} \tag{13}$$

Allen et al. [25] used one kind of rodlike particles (l/d = 1.2), and also proposed an empirical equation of friction factor of the packed bed (ε = 0.4), which is termed as "N-II" model:

$$A = 243 \tag{14}$$

$$B = \frac{6.93}{Re*^{0.12}} \tag{15}$$

It should be noted that the variety of aspect ratios of rodlike particles in both "N-I" and "N-II" models is much limited. To further develop the empirical equation of friction factors, more experiment data is needed. In this work, the pressure drop through the packed bed with height of 200–300 mm is measured, and then the friction factor is calculated based on the particle properties and porosity of bed shown in Table 1 and Table 2. To minimise the effect of initial packing conditions and avoid the horizontal alignment of particles in poured packing, only the packed bed formed by fluidised packing method is used. The value of A and B in Eq. (9) could be obtained by least square fitting of the curve of variation of friction factor with modified Reynolds number, as shown in Fig. 4. It shows that the friction factor decreases with modified Reynolds number. The value of A and B for all four kinds of rodlike particles is shown in Table 2. It shows that A increases with the aspect ratio of rodlike particles (i.e. the decrease of sphericity), but B is much less sensitive to the aspect ratio.

To improve the predictions of the model, three sources of experimental data are used:

Table 2
Physical properties of the particles and bed.

Label	d_V/mm	d_{SV}/mm	ϕ	ε	A	B
WS	2.14	1.77	0.826	0.401	178.2	2.4
WL	3.11	2.39	0.768	0.415	183.7	2.3
BS	4.74	3.38	0.713	0.549	281.1	2.4
BL	3.36	2.12	0.631	0.616	361.8	1.6

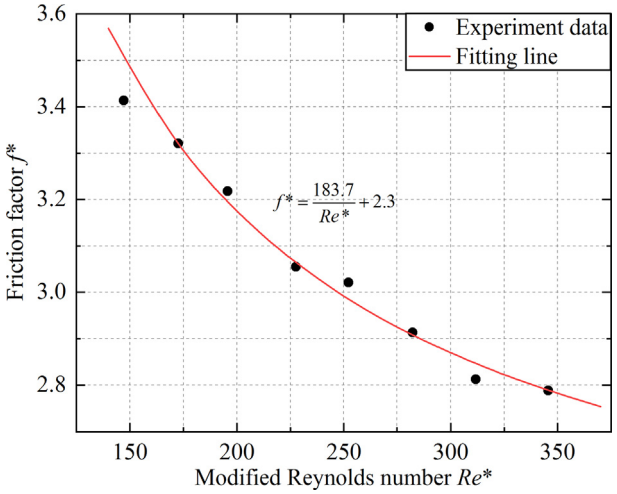

Fig. 4. The variation of friction factor with modified Reynolds number for particle WL.

(1) The friction factor of 6 kinds of rodlike particles used to fit the "N-I" and "N-II" models, including Pahl et al. [18] (l/d = 1.31, 3.81), Nemec & Levec [20] (l/d = 1.91, 2.94, 5.77), and Allen et al. [25] (l/d = 1.2). The value of A and B in Eq. (9) could be fitted from the variation of friction factor with modified Reynolds number.
(2) The friction factor of 4 kinds of rodlike particles (l/d = 1.02,1.25, 3.0, 3.59), which is re-calculated based on the pressure drop of fluid flow provided by Vollmari et al. [33]. However, their data showed that the friction factor f^* decreases with modified Reynolds number Re^* firstly, but then increased with Re^* sharply, which is contrary to the predictions of previous models. This might be caused by the effect of the gas distributor. Thus, the friction factor at high modified Reynolds number in Vollmari et al. [33] is not used in this work. The values of A and B in Eq. (9) could be fitted from the variation of friction factor with modified Reynolds number.
(3) the friction factor of 4 kinds of rodlike particles (l/d = 2.11, 3.23, 4.53, 7.34) in this work, as shown in Table 2.
(4) Meanwhile, to consider the effects of particle orientation on the packed bed, the equivalent sphericity Φ_{eq} is introduced for rodlike particles:

$$\phi_{eq} = \left(\frac{1}{3\sqrt{\phi_\perp}} + \frac{2}{3\sqrt{\phi}}\right)^{-1} \tag{16}$$

where $\Phi_\perp$ is the crosswise sphericity, namely the ratio between the cross-sectional area of the volume equivalent sphere and the projected cross-sectional area of the considered rodlike particle perpendicular to the fluid flow. The equivalent sphericity Φ_{eq} is also termed as Stokes' shape factor introduced by Ganser [45].

The variation of the friction factor with equivalent sphericity is shown in Fig. 5. The data points are scattered, which may be caused by the difference of the preparation methods to generate the packed bed between the sources of experimental data. By using least square fitting, the empirical equations of A and B could be given as:

$$A = \frac{150}{\phi_{eq}^{3.0}} \tag{17}$$

$$B = \frac{2.5}{\phi_{eq}^{-0.4}} \tag{18}$$

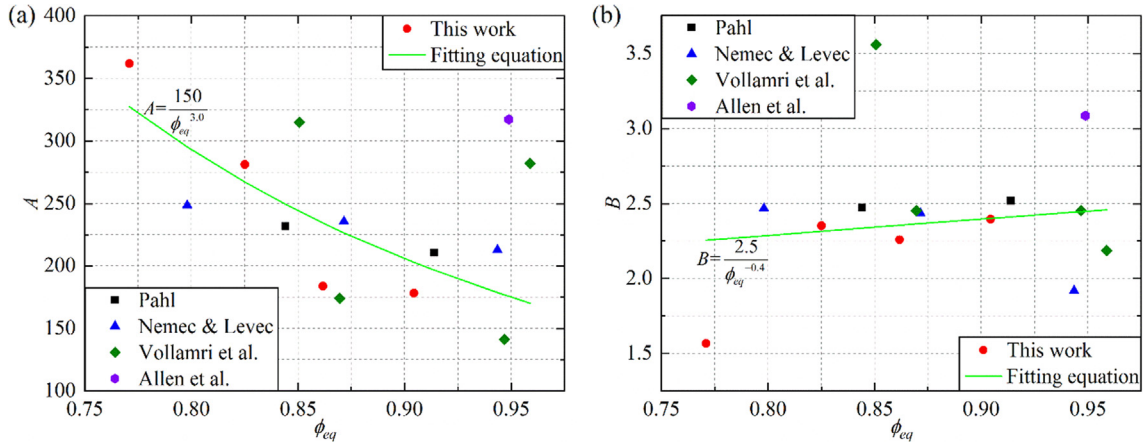

Fig. 5. Variation of A (a) and B (b) with equivalent sphericity.

Table 3
Relative deviation of the empirical correlations.

Model	Ergun Equation	N-II Model	N-I Model	This work
Relative deviation/%	29.49	33.47	19.65	12.85

To compare the accuracy of different empirical equations, the relative deviation of friction factor is calculated at each modified Reynolds number and then averaged, as shown in Eq. (19). The mean relative deviation of all kinds of rodlike particles is shown in Table 3. It shows that the predictions of new empirical correlation in this work are closer to the experimental results.

$$MRD = \frac{1}{N}\sum_{i=1}^{N}\frac{f_{i,calc}* - f_{i,exp}*}{f_{i,exp}*} \times 100\% \tag{19}$$

5. Conclusions

The packed bed of rodlike particles is explored by experimental method. The packed bed is generated by the poured packing method and fluidised packing method. The effect of aspect ratio of rodlike particles on the bed structure is quantified by the porosity and friction factor. The main results from the present study can be summarised as follows:

(1) With the increase of aspect ratio, the porosity in the packed bed firstly decreases and then increases, which is the result of the competition between the self-fitting effects and excluded effects.
(2) Compared to spherical particles, the packed bed of rodlike particles is more sensitive to the packing method.
(3) Based on the pore conduct model, a new empirical correlation is developed to predict the friction factor of the packed bed of rodlike particles with better accuracy, where the effect of particle orientation is considered with particle shape.

Acknowledgments

The authors are grateful to the National Natural Science Foundation of China (Grant No. 51806099) and Start-up Foundation for Introducing Talent of Nanjing Tech University (Grant No. 39802120) for the financial support of this work.

References

[1] J.V. Milewski, The combined packing of rods and spheres in reinforcing plastics, Ind. Eng. Chem. Prod. Res. Dev. 17 (1978) 363–366.
[2] M. Nardin, E. Papirer, J. Schultz, Contribution à l'etude des empilements au hasard de fibres et/ou de particules sphériques, Powder Technol. 44 (1985) 131–140.
[3] K.E. Evans, M.D. Ferrar, The packing of thick fibres, J. Phys. D Appl. Phys. 22 (1989) 354.
[4] J.G. Parkhouse, A. Kelly, The random packing of fibres in three dimensions, P R Soc-Math Phys. Sci. 451 (1995) 737–746.
[5] R.P. Zou, A.B. Yu, Evaluation of the packing characteristics of mono-sized non-spherical particles, Powder Technol. 88 (1996) 71–79.
[6] O. Rahli, L. Tadrist, R. Blanc, Experimental analysis of the porosity of randomly packed rigid fibers, Cr Acad Sci Ii B 327 (1999) 725–729.
[7] M. Novellani, R. Santini, L. Tadrist, Experimental study of the porosity of loose stacks of stiff cylindrical fibres: Influence of the aspect ratio of fibres, Eur. Phys. J. B 13 (2000) 571–578.
[8] W. Zhang, K.E. Thompson, A.H. Reed, L. Beenken, Relationship between packing structure and porosity in fixed beds of equilateral cylindrical particles, Chem. Eng. Sci. 61 (2006) 8060–8074.
[9] S.R. Williams, A.P. Philipse, Random packings of spheres and spherocylinders simulated by mechanical contraction, Phys. Rev. E 67 (2003) 051301.
[10] L. Pournin, M. Weber, M. Tsukahara, J.A. Ferrez, M. Ramaioli, T.M. Liebling, Three-dimensional distinct element simulation of spherocylinder crystallization, Granular Matter 7 (2005) 119–126.
[11] A. Wouterse, S. Luding, A.P. Philipse, On contact numbers in random rod packings, Granular Matter 11 (2009) 169–177.
[12] J. Zhao, S.X. Li, R.P. Zou, A.B. Yu, Dense random packings of spherocylinders, Soft Matter 8 (2012) 1003–1009.
[13] L. Meng, P. Lu, S. Li, J. Zhao, T. Li, Shape and size effects on the packing density of binary spherocylinders, Powder Technol. 228 (2012) 284–294.
[14] F. Doraia, M. Rolland, A. Wachs, M. Marcoux, E. Climent, Packing fixed bed reactors with cylinders: influence of particle length distribution, Proc. Eng. CHISA 2012 (42) (2012) 1335–1345.
[15] X.L. Deng, R.N. Dave, Dynamic simulation of particle packing influenced by size, aspect ratio and surface energy, Granular Matter 15 (2013) 401–415.
[16] W.G. Nan, Y.S. Wang, Y. Ge, J.Z. Wang, Effect of shape parameters of fiber on the packing structure, Powder Technol. 261 (2014) 210–218.
[17] W.G. Nan, Y.S. Wang, Y.W. Liu, H.P. Tang, DEM simulation of the packing of rodlike particles, Adv. Powder Technol. 26 (2015) 527–536.
[18] M.H. Pahl, Über die Kennzeichnung diskret disperser Systeme und die systematische Variation der Einflussgrössen zur Ermittlung eines allgemeingültigeren Widerstandsgesetzes der Porenströmung, University of Karlsruh, 1975.
[19] N. Rangel, A. Santos, C. Pinho, Pressure drop in packed shallow beds of cylindrical cork stoppers, Chem Eng Res Des 79 (2001) 547–552.
[20] D. Nemec, J. Levec, Flow through packed bed reactors: 1 Single-phase flow, Chem. Eng. Sci. 60 (2005) 6947–6957.
[21] R. Singh, R.P. Saini, J.S. Saini, Nusselt number and friction factor correlations for packed bed solar energy storage system having large sized elements of different shapes, Sol. Energy 80 (2006) 760–771.
[22] R. Escudié, N. Epstein, J.R. Grace, H.T. Bi, Effect of particle shape on liquid-fluidized beds of binary (and ternary) solids mixtures: segregation vs. mixing, Chem. Eng. Sci. 61 (2006) 1528–1539.

[23] B.Q. Liu, X.H. Zhang, L.G. Wang, H. Hong, Fluidization of non-spherical particles: Sphericity, Zingg factor and other fluidization parameters, Particuology 6 (2008) 125–129.
[24] E. Ozahi, M.Y. Gundogdu, M.O. Carpinlioglu, A modification on Ergun's correlation for use in cylindrical packed beds with non-spherical particles, Adv. Powder Technol. 19 (2008) 369–381.
[25] K.G. Allen, T.W. von Backstrom, D.G. Kroger, Packed bed pressure drop dependence on particle shape, size distribution, packing arrangement and roughness, Powder Technol. 246 (2013) 590–600.
[26] Y.J. Shao, B. Ren, B.S. Jin, W.Q. Zhong, H. Hu, X. Chen, C.F. Sha, Experimental flow behaviors of irregular particles with silica sand in solid waste fluidized bed, Powder Technol. 234 (2013) 67–75.
[27] W.Q. Zhong, Y. Zhang, B.S. Jin, M.Y. Zhang, Discrete element method simulation of cylinder-shaped particle flow in a gas-solid fluidized bed, Chem. Eng. Technol. 32 (2009) 386–391.
[28] J.E. Hilton, L.R. Mason, P.W. Cleary, Dynamics of gas–solid fluidised beds with non-spherical particle geometry, Chem. Eng. Sci. 65 (2010) 1584–1596.
[29] Z.Y. Zhou, D. Pinson, R.P. Zou, A.B. Yu, Discrete particle simulation of gas fluidization of ellipsoidal particles, Chem. Eng. Sci. 66 (2011) 6128–6145.
[30] B. Ren, W.Q. Zhong, Y. Chen, X. Chen, B.S. Jin, Z.L. Yuan, Y. Lu, CFD-DEM simulation of spouting of corn-shaped particles, Particuology 10 (2012) 562–572.
[31] B. Ren, W.Q. Zhong, B.S. Jin, Y.J. Shao, Z.L. Yuan, Numerical simulation on the mixing behavior of corn-shaped particles in a spouted bed, Powder Technol. 234 (2013) 58–66.
[32] T. Oschmann, J. Hold, H. Kruggel-Emden, Numerical investigation of mixing and orientation of non-spherical particles in a model type fluidized bed, Powder Technol. 258 (2014) 304–323.
[33] K. Vollmari, T. Oschmann, S. Wirtz, H. Kruggel-Emden, Pressure drop investigations in packings of arbitrary shaped particles, Powder Technol. 271 (2015) 109–124.
[34] K. Vollmari, R. Jasevičius, H. Kruggel-Emden, Experimental and numerical study of fluidization and pressure drop of spherical and non-spherical particles in a model scale fluidized bed, Powder Technol. 291 (2016) 506–521.
[35] W. Nan, Y. Wang, J. Wang, Numerical analysis on the fluidization dynamics of rodlike particles, Adv. Powder Technol. 27 (2016) 2265–2276.
[36] H. Ma, L. Xu, Y. Zhao, CFD-DEM simulation of fluidization of rod-like particles in a fluidized bed, Powder Technol. (2016).
[37] Y. He, F. Guo, Micromechanical analysis on the compaction of tetrahedral particles, Chem. Eng. Res. Des. 136 (2018) 610–619.
[38] N. Pratten, The precise measurement of the density of small samples, J. Mater. Sci. 16 (1981) 1737–1747.
[39] J. Heiskanen, Comparison of three methods for determining the particle density of soil with liquid pycnometers, Commun. Soil Sci. Plant Anal. 23 (1992) 841–846.
[40] A. Donev, I. Cisse, D. Sachs, E.A. Variano, F.H. Stillinger, R. Connelly, S. Torquato, P.M. Chaikin, Improving the density of jammed disordered packings using ellipsoids, Science 303 (2004) 990–993.
[41] I. Balberg, C.H. Anderson, S. Alexander, N. Wagner, Excluded volume and its relation to the onset of percolation, Phys. Rev. B 30 (1984) 3933–3943.
[42] W. Nan, Investigations on the Packing Structure and Dense Phase Transport Behaviour of Slender Particles, Phd thesis, Xi'an Jiaotong University, Xi'an, 2017.
[43] R.K. Niven, Physical insight into the Ergun and Wen & Yu equations for fluid flow in packed and fluidised beds, Chem. Eng. Sci. 57 (2002) 527–534.
[44] W.-C. Yang, Handbook of Fluidization and Fluid-Particle Systems, Marcel Dekker Inc, New York, 2003.
[45] G.H. Ganser, A rational approach to drag prediction of spherical and nonspherical particles, Powder Technol. 77 (1993) 143–152.